IMAGE PROCESSING FOR CHARACTERISATION OF SURFACES OF SUPERCONDUCTING RF CAVITIES

M. Wenskat, S. Aderhold, E. Elsen, S. Karstensen, F. Schlander and L. Steder,
DESY, Hamburg, Germany

Abstract

The 1.3 GHz superconducting rf-cavities for the International Linear Collider ILC are foreseen to operate at an average accelerating gradient of 31.5 MV/m. While an even higher field would be desirable it has been repeatedly observed [1–3] that surface structures in the range of a few microns to several millimeters may limit the performance of the cavities. With the introduction of the *Kyoto camera* [4] it has become possible to examine the inner surface of a 9-cell superconducting cavitiy after surface preparation. The high-resolution camera resolves structures down to 5 µm for properly illuminated surfaces and thus seems ideally suited to search for such structures. Meanwhile at DESY about 30 cavities have been inspected and first results have been presented [5–7]. Manual image taking and visual examination of the large picture inventory are time consuming and will no longer be practical for the large number of cavities foreseen for the European XFEL and eventually the ILC. The first experience in automated image acquisition using the OBACHT apparatus and automated image processing are the topic of this paper.

AUTOMATED OPTICAL INSPECTION

A fully automated robot for optical inspection has been developed at DESY. The *Optical Bench for Automated Cavity inspection with High resolution and short Timescales* (OBACHT) uses linear and rotational drives to position the camera inside the cavity, *cf.* Fig. 1. The high-resolution camera resolves structures down to 5 µm for properly illuminated surfaces; a single image consists of 3488×2616 pixels. The power of the method is illustrated in Fig. 2, which contrasts a high-resolution image of a welding seam and a candidate defect location with an earlier image from approximately the same area taken with a boroscope that is typically used to examine the quality of the welding seam proper. A total of 2790 images are taken per cavity to map out the equator between two half-cells (9×90 images), the two adjacent heat-affected zones (2×9×90 images) and the iris between two elliptical cells and the beam pipe (10×36 images). Including time for mounting of the cavity and calibration the entire procedure for image taking and data storage takes about 10 h. The longitudinal and radial positional accuracy of the motor system is in the order of a few µm. The high reproducibility of the positioning systems enables re-inspection of a cavity and of specific locations so that e.g. suspicious locations can be traced throughout various stages of the treatment process.

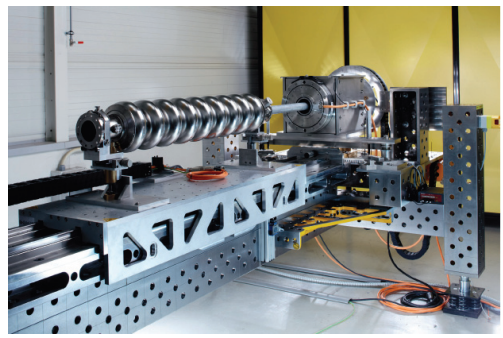

Figure 1: The robot OBACHT for automatic scan of cavity inner surfaces.

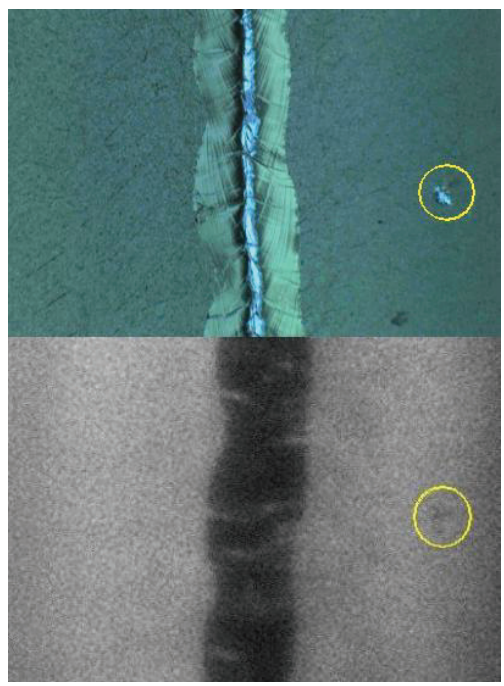

Figure 2: Image of a welding seam taken with OBACHT (top) and with a boroscope (bottom), courtesy E.Zanon. A suspicious spot (yellow circle) is indicated in both images.

The high accuracy also enables a geometrical survey of the cavity and the individual cells. To date OBACHT has been used to inspect 11 cavities in the fully automated mode.

ISBN 978-3-95450-115-1

The linear and rotational drives are controlled by a PLC system, which itself is steered from a LabVIEW [8] environment. Other features such as camera focal positioning, spot illumination and image acquisition are also implemented in Labview.

The stored images are filed and processed offline for feature extraction. The control of the tools and the monitoring is described in [9].

AUTOMATED IMAGE PROCESSING

First attempts of developing an algorithm that analyses an image and classifies the surface properties have been made [10]. Such an algorithm is able to measure the surface roughness and to histogram feature sizes over a range of scales from several 10 µm to several millimeters. It also distinguishes welding seam from the surrounding bulk niobium. Defect recognition, however, requires the detection of rare and lone irregularities that are difficult to discern from the surrounding bulk material. Nonetheless, it is typically at the position of these defects, i.e. foreign material enclosures or geometrical deformations leading to large field enhancements, where eventually a quench occurs. An algorithm based on the method of eigenfaces [11] has been implemented and has been used to recognize similarities between surface features. Consider $I(x, y)$ as the grey-scale intensity encoding of a pixel at position (x, y) of a square image Γ_i consisting of $N \times N$ pixels. The same array can be interpreted as a vector with N^2 components, i.e. a point in N^2-dimensional space. For a cavity surface area this space is not uniformly populated. In fact, the challenge of finding similarities between image areas is to determine the subspace in which the intensity only fluctuates around the expected greyscale value according to the manufacturing variation. The method applied here employs a principal component analysis based on a training sample of M cavity images $\Gamma_1, \Gamma_2, \ldots, \Gamma_M$.

The mean image $\bar{\Gamma}$ and its variance C can be readily calculated

$$\bar{\Gamma} = \frac{1}{M} \sum_{i=1}^{M} \Gamma_i \tag{1}$$

$$C = \frac{1}{M} \sum_{i=1}^{M} (\Gamma_i - \bar{\Gamma})(\Gamma_i - \bar{\Gamma})^T \tag{2}$$

which again represent arrays of size $N \times N$. The eigenvectors of the matrix C can be used to decompose the image space in terms of its most relevant properties, i.e. the eigenfaces. Typically only a small number of eigenvectors are needed to describe the relevant features of the image. The selection of a minimal set of eigenvectors which best describe the images reduces the dimensionality of the search.

Any irregularity of the surface, such as a defect or enclosure, deviates from the typical surface of the training sample and hence would be identified by distinctly different coordinates. The distance so measured can be used to extract such features.

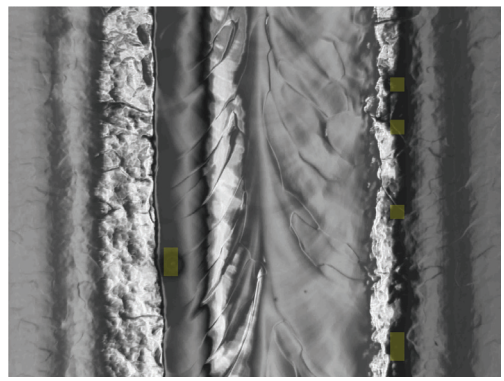

Figure 3: Image of a welding seam in cavity *AC127*. The output of the eigenfaces algorithm is indicated by the yellow squares. Two defects (two yellow squares on the left) have been identified, five other spots where falsely classified as an irregularity (shown as the 5 yellow squares on the right side of the welding seam).

IMPLEMENTATION AND RESULTS

The algorithm has been tested on cavity *AC127* for which an extended set of measurements is available. Before assembly into a cryomodule the cavity could be operated at up to 28 MV/m at a Q_0 of 1.5×10^{10}. During operation at FLASH, a degradation to 19 MV/m at Q_0 of 2.5×10^9 was found. After the upgrade of the FLASH facility at DESY, the module was exchanged and the cavity could be extracted and tested again in the vertical test stand. These tests confirmed the gradient degradation and the cavity was found to be quench limited. A second sound measurement realised in the vertical test stand at DESY [12] located the quench in cell number 2 at 270 degrees in four modes. The optical inspection revealed a spot which resembled a burst of debris.

The image of *AC127* seen in Fig. 3 was used to test the algorithm described above. The image has been partitioned into squares of 101 pixels side length, leaving 34*26 square to analyse per image. As a training set the 34 squares of the top row in the image have been used. Fig. 4 (left) shows the area of the defect while Fig. 4 (right) shows the same region after subtracting the ten leading eigenvectors weighted with the appropriate eigenvalues. The signal to noise ratio (SNR) increases from 13.8 dB to 16.2 dB for the squares including the defect. At the same time, the SNR for the whole image increases by 0.7 dB indicating that the essential features are described. Irregularities in the image are detected by introducing a normalized distance: the mean Euclidean distance (centre of gravity) and its variance is calculated for all squares. If a square is more than 3.5 σ away from the centre of mass, it is marked as an irregularity. In Fig. 3, the output of the algorithm is shown. Two squares containing the defect were found but also five

ISBN 978-3-95450-115-1

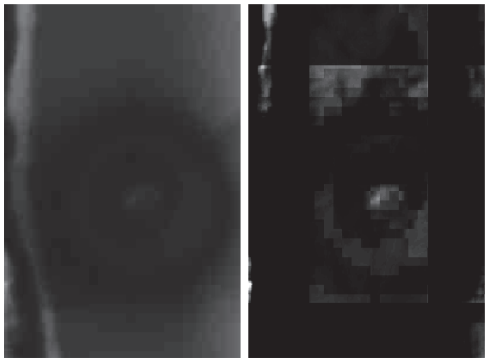

Figure 4: The original cross section of the defect area in cavity *AC127* (left) and after subtraction of the ten most relevant eigenvector weighted with the eigenvalues (right).

squares which do not contain any defect. The reason for the false classification could be traced to the chosen training set. All falsely classified squares contain the same light reflection pattern which was not well represented in the original training set.

SUMMARY AND OUTLOOK

The optical inspection robot OBACHT at DESY enables the swift inspection of cavities with high precision and efficiency. Tools for automatic classification of the surface properties and recognition of defects are being developed and will be improved as feature variations are better understood. Using the ILC-HiGrade cavities, which will be produced alongside the batch of cavities for the European XFEL, a large image database with a significant statistics will become available. Algorithms for analysis of this inventory are being developed.

ACKNOWLEDGMENT

The work is supported by the 7th Framework Programme ”Construction of New Infrastructures - Preparatory Phase”, ILC-HiGrade, contract number 206711.

REFERENCES

[1] Y. Xie et al., "Relationship between defects pre-heating and defects size", Proc. of the 14th Workshop on RF Superconductivity, Berlin, Germany 2009

[2] K. Watanabe, "Review of optical inspection methods and results", Proc. of the 14th Workshop on RF Superconductivity, Berlin, Germany 2009

[3] V. Shemelin and H. Padamsee, "Magnetic field enhancement at pits and bumps on the surface of superconducting cavities", TTC-Report 2008-07

[4] Y. Iwashita et al., "Development of high resolution camera for observations of superconducting Cavities", Phys. Rev. ST. Accel. Beams 11, 093501 (2008)

[5] S. Aderhold, "Optical inspection of SRF cavities at DESY", Proc. of the 14th Workshop on RF Superconductivity, Berlin, Germany 2009

[6] S. Aderhold, "Large Grain Cavities: Fabrication, RF Results and Optical Inspection", Proc. of the 15th Workshop on RF Superconductivity, Chicago, Illinois, USA 2011

[7] W.-D. Möller, "Review of results from temperature mapping and subsequent cavity inspection", Proc. of the 14th Workshop on RF Superconductivity, Berlin, Germany 2009

[8] LabVIEW Version 2011, Austin, Texas: National Instruments

[9] L. Steder, "Measurement Manual for OBACHT", ILC HiGrade Report 2012-001-1

[10] M. Wenskat, "Automated Optical Inspection - Image analysis and defect recognition", LCWS11, International Workshop on Future Linear Colliders, Granada, Spain

[11] L. Sirovich and M. Kirby, "Low-dimensional procedure for the characterization of human faces," J. Opt. Soc. Am. A 4, 519-524 (1987)

[12] F. Schlander, E. Elsen, D. Reschke, "Second Sound as an automated Quench Localisation Tool at DESY", Proc. of the 15th Workshop on RF Superconductivity, Chicago, Illinois, USA 2011